RESEARCH ARTICLE

Kinetic comparison of isomeric oligo(ethylene oxide) (meth)acrylates: Aqueous polymerization of oligo(ethylene oxide) methyl ether methacrylate and methyl 2-(oligo (ethylene oxide) methyl ether)acrylate macromonomers

Michael R. Martinez¹ | Sylwia Dworakowska^{1,2} | Adam Gorczyński^{1,3} | Grzegorz Szczepaniak¹ | Ferdinando De Luca Bossa¹ | Krzysztof Matyjaszewski¹ •

Correspondence

University, Poznań, Poland

Krzysztof Matyjaszewski, Department of Chemistry, Center for Macromolecular Engineering, Carnegie Mellon University, 4400 Fifth Avenue, Pittsburgh, PA 15213, USA.

Email: km3b@andrew.cmu.edu

Funding information

National Science Foundation; Carnegie Mellon University

Abstract

The photoinduced energy/electron transfer-reversible addition-fragmentation chain transfer (PET-RAFT) polymerizations of oligo(ethylene oxide) monomethyl ether methacrylate (OEOMA, also known as poly[ethylene glycol] methyl ether methacrylate, PEGMA) and isomeric methyl 2-(oligo(ethylene oxide) methyl ether)acrylate (20EOAM) macromonomers with OEO average degree of polymerization of 22 or 45 were conducted in aqueous media to provide insight into the effect of monomer structure on grafting-through RAFT of 1,1-disubstituted acrylic macromonomers. The polymerizations of all four monomers reached nearly quantitative conversion. The longer macromonomers polymerized faster than the shorter ones within the same monomer class. The OEO side chain at the α (i.e., 2-) position of isomeric acrylates significantly slowed RAFT polymerization in comparison with OEO ester side chain of methacrylates.

KEYWORDS

bottlebrushes, kinetics, macromonomer, methacrylate, PET-RAFT

1 | INTRODUCTION

Molecular bottlebrushes are comb copolymers with sidechains densely grafted to/from a central polymer backbone. 1-7 Steric hindrance caused by dense packing of side chains along a polymer backbone leads to short-range rigidity and rod-like topologies at high aspect ratio. 8.9 Densely grafted molecular bottlebrushes have

Dedicated to Professor Klaus Müllen on the occasion of his 75th birthday.

higher molecular weights between entanglements in the melt, leading to lower intrinsic viscosities and lower moduli than conventional polymer chains with small substituents. ^{10–12} These properties enabled use of molecular bottlebrushes as specialty materials, such as lubricants, ^{13–15} nanomaterials, ^{16–18} surfactants, ^{19–21} drug delivery vehicles, ^{22–24} and as supersoft elastomers with tissue-like mechanical properties. ^{25–30}

Bottlebrushes can be prepared by grafting small monomers from a multi-functional initiator backbone in

This is an open access article under the terms of the Creative Commons Attribution-NonCommercial-NoDerivs License, which permits use and distribution in any medium, provided the original work is properly cited, the use is non-commercial and no modifications or adaptations are made.

© 2022 The Authors. *Journal of Polymer Science* published by Wiley Periodicals LLC.

J Polym Sci. 2022;60:1887–1898. wileyonlinelibrary.com/journal/pol 1887

¹Department of Chemistry, Center for Macromolecular Engineering, Carnegie Mellon University, Pittsburgh, Pennsylvania, USA

²Department of Biotechnology and Renewable Materials, Faculty of Chemical Engineering and Technology, Cracow University of Technology, Cracow, Poland ³Faculty of Chemistry, Adam Mickiewicz

the "grafting-from" approach, 15,31-35 coupling chains onto a functionalized backbone via the "grafting-onto" approach, 36,37 and by the polymerization of macromonomers in the "grafting-through" approach. 38-43 Synthesis of molecular bottlebrushes by grafting-through of vinyl macromonomers using reversible deactivation radical polymerization (RDRP) provides densely grafted bottlebrushes with side chains on every other carbon along the backbone. However, grafting-through RDRP of macromonomers via RDRP is challenging due to the low concentration of polymerizable vinyl groups, steric hindrance of long chain substituents and high viscosity. The dilution leads to a slower rate of polymerization due to lower concentration of polymerizable vinyl groups (monomer) and dormant chain ends (alkyl halides in ATRP or chain transfer agents [CTA] in a RAFT polymerization).44 Grafting-through polymerization of methacrylic macromonomers with an initial monomer concentration ([M]₀) close to the equilibrium monomer concentration ([M]_{eq}) may proceed slowly and plateau at a dead-end monomer concentration ([M] $_{\infty}$) close to the [M] $_{\text{ea}}$.

Molecular bottlebrushes with oligo(ethylene oxide) (OEO, also known as poly[ethylene glycol], PEG) side chains are of particular interest due to their potential biomedical applications in drug/gene delivery, anti-fouling, electronics, and thermoresponsive materials. 19,20,48-54 The majority of bottlebrushes with oligo(ethylene oxide) side chains were prepared by RDRP using graftingthrough polymerization of macromonomers. 43,46,50,51,55-59 OEO macromonomers are commonly prepared by esterification between the mono-OH capped OEO methyl ether and the acid functional group attached to styrenes, acrylates, or methacrylates. Oligo(ethylene oxide) monomethyl ether methacrylate (OEOMA) macromonomers have a methyl substituent in the a position of the acrylate functional group, and a long oligo(ethylene oxide) ester side chain (Figure 1). The final bottlebrush yield in OEOMA polymerizations with long sidechains is limited by the equilibrium monomer concentrations. 43,46 Polymerization yields increase at higher [M]0, higher pressure, lower temperature, and in aqueous media. 43,47 Depolymerizations of P(OEOMA) bottlebrushes into macromonomers by RAFT were also reported. 46,60

This manuscript investigates the aqueous grafting-through polymerization of commercially available methacrylic OEO $_{22}$ MA and OEO $_{45}$ MA macromonomers, and "inverted" methyl 2-(oligo(ethylene oxide) methyl ester)acrylate (2OEOAM) macromonomers of identical average OEO lengths (Figure 1). The 2OEOAM macromonomers were prepared in a biphasic solution (NaOH $_{aq}$ /CH $_{2}$ Cl $_{2}$) with methyl α -(bromomethyl)acrylate, oligo(ethylene glycol) monomethyl ether and tetrabutylammonium bromide as a phase-transfer

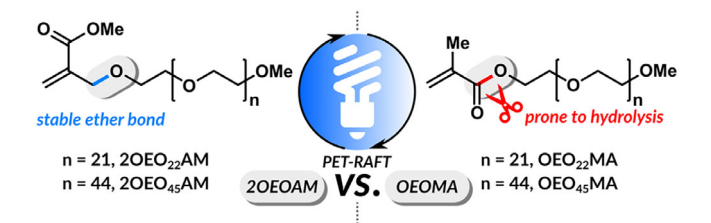


FIGURE 1 Oligo(ethylene oxide) monomethyl ether methacrylate and methyl 2-(oligo(ethylene oxide) methyl ether) acrylate macromonomers with n=21 and 44 investigated in this study

catalyst. The synthesis is discussed in detail in the Supplementary Information. The two "inverted" 20EOAM macromonomers consisted of an OEO sidechain tethered to the acrylate functional group, and subsequent polymer backbone, by the methyl ether bond in the α -position. The attachment of the OEO sidechain via an ether bond should improve the hydrolytic stability of the P (20EOAM) bottlebrushes, relative to standard POEOMA bottlebrushes. Crosslinkers based upon bifunctional 20EO_nAM macromonomers are used as precursors to commercial ChemMatrix® Resins, which have applications in solid phase peptide synthesis. 61,62 This is the first reported grafting-through polymerization of OEOMA with long sidechains under oxygen tolerant conditions, and the first RDRP of a 2-(oligo(ethylene oxide) methyl ether)acrylate macromonomer.

The aqueous photoinduced electron/energy transfer RAFT (PET-RAFT) grafting-through polymerization of four macromonomers bearing oligo(ethylene glycol) grafts was compared using a tris(bipyridine)ruthenium (II) chloride (Ru[bpy]₃Cl₂) catalyst under blue light irradiation without additional reducing agents or prior degassing, using trithiocarbonate CTAs. 63–65 The kinetics of PET-RAFT polymerizations were followed until the reactions reached >90% conversion by ¹H NMR to provide insight into how structural differences in substituents surrounding the olefin could affect grafting-through RAFT polymerizations of 1,1-disubstituted vinyl OEO macromonomers.

2 | RESULTS AND DISCUSSION

Aqueous PET-RAFT of oligo(ethylene oxide) monomethyl ether methacrylate (OEOMA) and an isomer with "inverted" arrangements of substituents, methyl 2-(oligo (ethylene oxide) monomethyl ether)acrylate (2OEOAM) macromonomers were conducted to follow the kinetics of their polymerization. The data is discussed using the naming format "[Molecular weight][Olefin structure]-[ppm Ru(bpy) $_3$ Cl $_2$]." The shorter OEO $_{22}$ MA

FIGURE 2 Photoinduced energy/electron transfer-reversible addition-fragmentation chain transfer polymerization of OEO₂₂MA with trithiocarbonate 4-((([2-carboxyethyl]thio)carbonothioyl)thio)-4-cyanopentanoic acid

macromonomer corresponds to the label 1KMA, the longer OEO₄₅MA corresponds to 2KMA, the inverted 2OEO₂₂AM is 1KAM, and the longer inverted 2OEO₄₅AM macromonomer is referred to as 2KAM. The experiment 1KMA-426-44 is given the additional -44 post-script to denote the higher target DP than the other experiments in this manuscript.

2.1 | Polymerization of OEO₂₂MA

Α trithiocarbonate 4-((([2-carboxyethyl]thio)carbonothioyl)thio)-4-cyanopentanoic acid (TTC) were tested in the polymerization of OEO₂₂MA with 426 ppm Ru(bpy)₃Cl₂ catalyst relative to monomer (Figure 2). It should be noted that the concentration of catalyst is on the order of a micromolar concentration due to the dilute nature of macromonomer polymerizations, and ppm is given relative to the concentration of monomer. The polymerization was conducted at an initial monomer concentration $[M]_0 = 88 \text{ mM}$ in a D_2O/DMF cosolvent solution (D₂O/DMF/monomer 71/20/9 v/v%), with no additional buffers or reducing agents. Macromonomer conversion was measured by the decrease of intensity of vinyl proton signal relative to the total signal of the methoxy protons in the side chains in the kinetic samples taken from the crude reaction mixture (Figure 3) (Figure S7).

The polymerization proceeded with linear first order kinetics until near-quantitative conversion was reached in 20 h. The $M_{n,\mathrm{GPC}}$ versus conversion plot showed that polymerization 1KMA-426-44 maintained control at lower conversion, but eventually lost control near the end of the polymerization as evidenced by the increase in dispersity of the product. It should be noted that the molecular weight of the crude polymerization products

were measured relative to linear poly(methyl methacrylate) (PMMA) standards in DMF, which underestimates the molecular weight of molecular bottlebrushes synthesized in this manuscript.⁶⁶

Oxygen concentration measurements were collected for model experiments with identical conditions as experiment 1KMA-426-44 (i.e., same [M]₀, solvent composition, and light source) with and without the 426 ppm Ru [bpy]₃Cl₂ photocatalyst to provide insight into the oxygen degassing mechanism. Irradiation of the reaction with no Ru(bpy)₃Cl₂ consumed oxygen by a photoiniferter process in absence of additional additives within 25 min, which contributed to oxygen degassing by a "polymerization-through oxygen" mechanism (Figure 4). The TTC/Ru(bpy)₃Cl₂ CTA/catalyst system increased the rate of oxygen consumption such that all oxygen was removed within 2.5 min of irradiation (Figure 4).

PET-RAFT with Ru(bpy)₃Cl₂ can generate the chainend radical under blue light irradiation by energy transfer between the excited photocatalyst and RAFT agent (Figure 5A). The excited Ru(bpy)₃Cl₂ catalyst reduces oxygen to a superoxide (O2 •) by an oxidative quenching mechanism (Figure 5B). 63,72-74 In aqueous solution, superoxide can be protonated to hydroperoxyl (HO2*, pKa = 4.8). Both HO₂ and superoxide were reported to disappear by second order processes in aqueous solutions. 75,76 The HO₂ can undergo disproportionation by reactions listed in Equations 1 and 2,75,77 to form hydroxyl radicals capable of initiating new chains and degassing by a "polymerization through oxygen" approach. 78,79 Indeed, we attempted RAFT polymerizations of OEO₂₂MA in a dimethyl sulfoxide/water solution without prior degassing and observed retardation and poor reaction control, presumably because initiation by peroxide species competed with oxidation of DMSO.

$$2HO_2 \cdot \to H_2O_2 + O_2,$$
 (1)

$$O_2^{\bullet -} + H_2O_2 \to HO^{\bullet} + OH^- + O_2.$$
 (2)

Subsequent polymerizations used a higher [TTC] at a lower molar ratio of $[OEO_{22}MA]$:[TTC] = 22/1 to improve control, with different loadings of $Ru(bpy)_3Cl_2$ (Table 1).

 ${
m OEO_{22}MA}$ polymerization with 852 ppm catalyst reached 68% conversion within the first hour of polymerization, then slowly proceeded to 84% conversion in 20 h (Figure 6). The dispersity of the product was low despite the retardation in reaction rate observed after the first hour (Figure 6). Progressively lowering catalyst loadings from 426 to 107 ppm did not significantly affect yield. The polymerizations reached >90% monomer conversion after 20 h without a compromise in polymerization

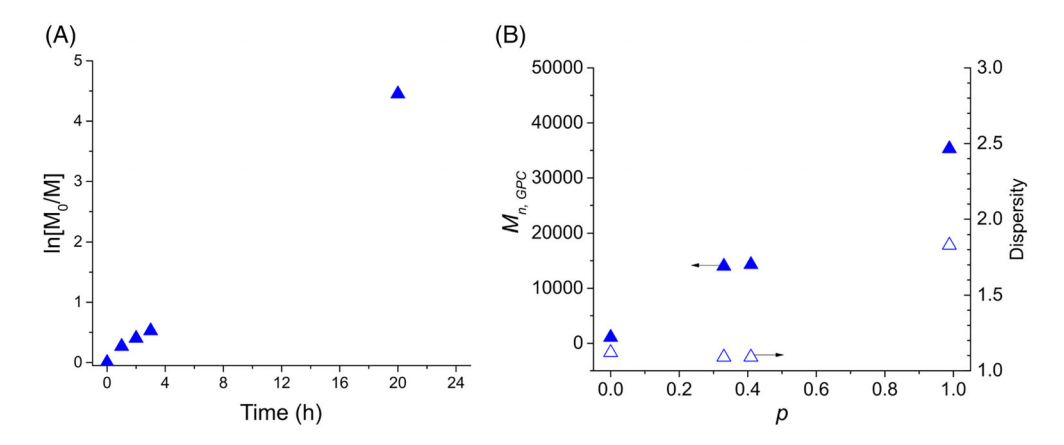


FIGURE 3 Photoinduced energy/electron transfer-reversible addition-fragmentation chain transfer polymerizations of OEO₂₂MA with trithiocarbonate 4-((([2-carboxyethyl]thio)carbonothioyl)thio)-4-cyanopentanoic acid (TTC) catalyzed by 426 ppm Ru[bpy] $_3$ Cl $_2$ in a 71/20 v/v% D $_2$ O/DMF cosolvent mixture. (A) First order kinetic plot; (B) M $_{n,GPC}$ and dispersity versus conversion. Molecular weight is given relative to linear PMMA standards in DMF. Reactions were performed at room temperature under 6.5 mW/cm 2 of blue light using [OEO $_{22}$ MA]:[TTC]:[Ru [bpy] $_3$ Cl $_2$] = 44/1/0.0188. The reaction temperature was 35–36°C with blue light irradiation

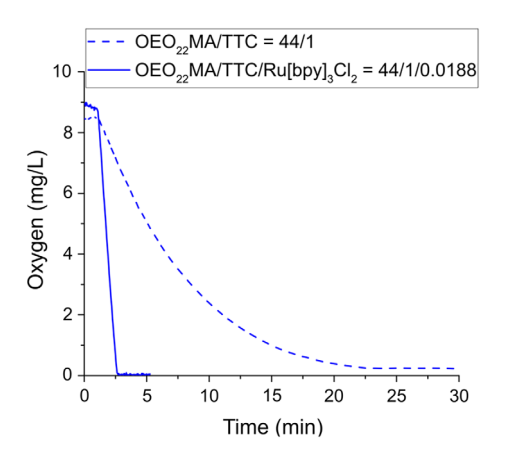
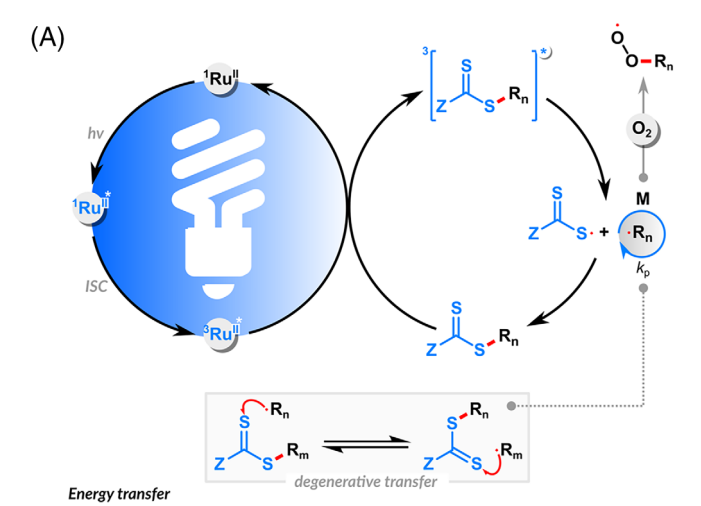


FIGURE 4 Oxygen content measurements of 1KMA-426-44 polymerizations with and without Ru(bpy) $_3$ Cl $_2$. Reactions were performed under blue light irradiation ($\lambda=465$ nm, 6.5 mW/cm 2) using [OEO $_{22}$ MA]:[TTC]:[Ru(bpy) $_3$ Cl $_2$] = 44/1/0.0188 or [OEO $_{22}$ MA]:[TTC] = 44/1. The reaction temperature was 35°C. The oxygen content measurements are calibrated against an OEO $_{22}$ MA solution in D $_2$ O ([M] $_0$ = 88 mM) bubbled with nitrogen for 20 min as the zero standard, and an OEO $_{22}$ MA solution in D $_2$ O ([M] $_0$ = 88 mM) sparged with air for 20 min as the oxygen-saturated standard

control. Similar trends in the first order kinetic plots were observed, where the reactions had a fast initial rate of polymerization which slowed until the reactions reached near completion. The polymerizations displayed acceptable control despite the high catalyst concentrations, with all polymerizations achieving >90% conversion in 20 h with bottlebrush dispersity below 1.3 (Figure 6). The $M_{n,\mathrm{GPC}}$ versus conversion plots had a linear increase in $M_{n,\mathrm{GPC}}$ with conversion until an apparent molecular weight of ~20,000 was obtained at ~60% conversion.



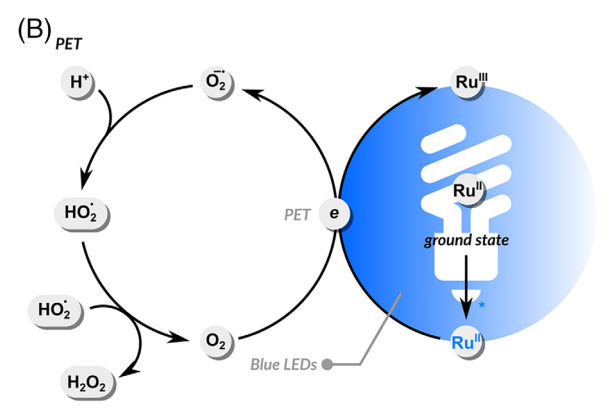


FIGURE 5 Catalytic cycle for (A) Photoinduced energy/ electron transfer-reversible addition-fragmentation chain transfer and (B) removal of oxygen by oxidative quenching using Ru(bpy)₃Cl₂ as the photocatalyst under blue light irradiation

It should be noted that tertiary trithiocarbonate RAFT have poor photostability after prolonged blue light

TABLE 1 Photoinduced energy/electron transfer-reversible addition-fragmentation chain transfer polymerization of OEO₂₂MA at 88 mM^a

Experiment	[OEO ₂₂ MA]/[CTA]/[Ru(bpy) ₃ Cl ₂]	$[Ru(bpy)_3Cl_2][\mu M, (ppm)]^b$	<i>t</i> (h)	p ^c	$M_{n, ext{th}}^{ ext{d}}$	$M_{n,\mathrm{GPC}}^{\mathbf{e}}$	$\boldsymbol{\mathit{D}}^{\mathbf{e}}$
1KMA-426-44	44/1/0.0188	38, (426)	20	0.99	46,800	35,300	1.83
1KMA-852	22/1/0.0188	75, (852)	20	0.84	20,000	20,400	1.20
1KMA-426	22/1/0.0094	38, (426)	20	0.95	22,600	20,400	1.23
1KMA-213	22/1/0.0047	19, (213)	20	0.93	22,200	20,100	1.22
1KMA-107	22/1/0.0023	9.2, (107)	20	0.93	22,200	20,000	1.22
1KMA-24	22/1/0.00051	2.1, (23)	24	0.94	22,400	18,600	1.52
1KMA-14	22/1/0.00031	1.2, (14)	24	0.93	22,200	23,400	1.53
1KMA-4	22/1/0.000103	0.4, (4.7)	24	0.89	21,200	26,700	1.41

^aTTC is the CTA. Solvent = 20/71% DMF/D₂O. Reactions were started upon exposure to blue light ($\lambda = 465$ nm, 6.5 mW/cm²) and were not degassed. The reaction temperature was 35°C, with a total volume of 3.25 ml. The reactions were conducted in sealed 1-dram vials.

^eFound by DMF GPC and is given relative to linear PMMA standards.

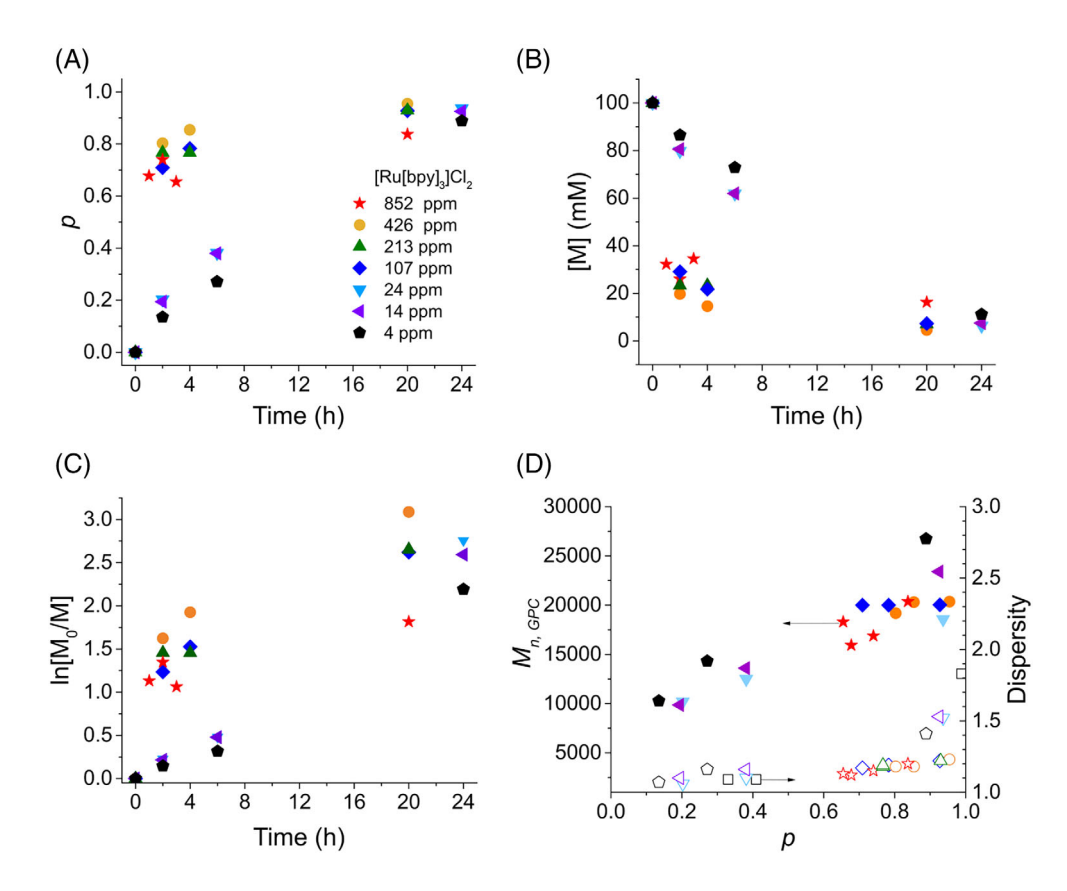


FIGURE 6 Photoinduced energy/electron transfer-reversible addition-fragmentation chain transfer polymerizations of $OEO_{22}MA$ with trithiocarbonate 4-((([2-carboxyethyl]thio)carbonothioyl)thio)-4-cyanopentanoic acid catalyzed by $Ru(bpy)_3Cl_2$ in a D_2O/DMF cosolvent system. (A) Kinetic plot of conversion versus reaction time. (B) Kinetic plot of monomer concentration versus time. (C) First order kinetic plot. (D) Molecular weight and dispersity versus conversion plot. The molecular weight of all samples are given relative to linear PMMA standards in DMF. Reactions were performed under 6.5 mW/cm² of blue light using $[OEO_{22}MA]$:[TTC]: $[Ru(bpy)_3Cl_2] = 22/1$ with the ppm of $Ru(bpy)_3Cl_2$ between 4–852 ppm. The reaction temperature was 35°C with blue light irradiation ($\lambda = 465$ nm, 6.5 mW/cm²)

irradiation.⁸⁰ The chain end could degrade to thiyl radicals by analogy to the photolytic degradation of TTC CTA's under UV irradiation.⁸¹ The hydrolysis of the

4-cyanopentanoic acid R- group to 4-amidopentanoic acid was also reported.⁸² Indeed, we observed negligible shift towards higher molecular weight at high conversion,

^bppm is reported relative to the equivalents of monomer by [mol Ru(bpy)₃Cl₂]/[mol OEO₂₂MA] \times 10⁶.

^cConversion determined by ¹H NMR (Supplementary Information).

 $^{^{}d}M_{
m n,th} = {
m m_{OEOMA}} \times {
m [OEOMA]/[CTA]} \times p + {
m m_{CTA}}.$

TABLE 2 Photoinduced energy/electron transfer-reversible addition-fragmentation chain transfer polymerization of oligo(ethylene oxide) macromonomers with Ru catalyst under blue light irradiation^a

Experiment	Monomer	$[M]_0$ (mM)	<i>t</i> (h)	$p^{\mathbf{b}}$	$k_{\mathrm{p,app}}^{}\mathrm{c}}(\mathrm{h}^{-1})$	$M_{n,\mathrm{GPC}}^{}$	$\boldsymbol{\mathit{D}}^{d}$	φ _{MM} (%) ^e	φ _{Olig} (%) ^e	φ _{BB} (%) ^e
1KMA-107 ^f	OEO ₂₂ MA	88	48	0.99	0.16	18,600	1.27	4	2	94
1KAM-94	2OEO ₂₂ AM	100	72	0.54	0.03	13,600	1.15	45	4	51
2KMA-94	OEO ₄₅ MA	100	24	>0.99	1.14 ^g	68,200	2.18	2	3	95
2KAM-94	2OEO ₄₅ AM	100	72	0.57	0.04	22,200	1.13	59	5	36
1KAM-94-2x	2OEO ₂₂ AM	200	68	0.96	0.07	14,500	1.34	5	8	87
2KAM-94-2x	2OEO ₄₅ AM	200	68	>0.99	0.12	31,800	1.32	5	4	91

^aConditions: [M]/[TTC]/[Ru(bpy)₃Cl₂] = 25/1/0.00234. Solvent = 20 vol% DMF and the remaining volume was D₂O. Reaction started upon exposure to blue light ($\lambda = 465 \text{ nm}$, 6.5 mW/cm²) without prior degassing. The reaction temperature was 35°C.

with the majority of new polymer formation appearing as low molecular weight oligomers (Figure S16).

The bottlebrushes produced using conditions 1KMA-4, IKMA-14, and 1KMA-24 had high dispersity above 1.5. The GPC traces in Figure S16 shows that the peak-average molecular weight of these reactions was higher than those with high catalyst loadings, however there were also more low molecular weight oligomers, leading to an overall high dispersity in the final sample. The higher peak-average molecular weight may be rationalized by a decreased contribution of oxygen removal by oxygen reduction with the [Ru(bpy)₃Cl₂] catalyst, and an increase in contribution of oxygen removal through the polymerization-through oxygen approach by direct photolysis of the TTC. Reactions degassed by latter approach sacrifice a portion of TTC to consume oxygen, which leads to lower initiation efficiency. The polymerizations were still slow, which led to CTA decomposition and oligomerization after prolonged blue light irradiation. Thus, the reactions with low concentration of photocatalyst had higher dispersity because of lower initiation efficiency and degradation of the TTC consistent with the other polymerizations in this manuscript. Despite these challenges, the polymerizations with low [Ru (bpy)₃Cl₂] reached comparable yields close to 90% conversion after 24 h with catalyst loadings as low as 4 ppm.

The polymerization with OEO₂₂MA was repeated until the reaction reached near quantitative conversion by ¹H NMR (1KMA-107, Table 2). The repeated polymerization had a consistent trend with the trials in Table 1, with a faster initial rate of polymerization followed by a slower second stage until the polymerization reached near quantitative conversion (Figure 7, Table 2). The gel permeaction chromatography (GPC) traces also showed

negligible increase in molecular weight with conversion, with low molecular weight tailing overlapping with the remaining macromonomer. The dispersity of the bottle-brushes remained close to 1.3 despite the oligomers visible in the GPC trace (Figure 8).

2.2 | Grafting-through polymerization of isomeric OEO macromonomers

The placement of the OEO functional group at the α-position could influence thermodynamic polymerizability and kinetic reactivity, relative to OEOMA. Bulky substituents reduce thermodynamic and kinetic favorability of radical polymerizations of 1,1-disubstituted monomers.^{83,84} Bulkier α-substituted acrylates had lower ceiling temperatures and slower rates of polymerization than less sterically hindered monomers, as reported in comparison of methyl acrylate, methyl methacrylate, and methyl 2-ethylacrylates.^{83–85} An interesting exception was observed in the conventional radical polymerization (RP) of 2-(alkyoxymethyl) acrylates. RP of 2-(alkyoxymethyl) acrylates were reported to be faster than RP of methyl methacrylate under identical conditions, however the isolated polymers had lower molecular weights. 86 RP of methyl 2-(npropyloxymethyl) acrylate, methyl 2-(n-butyloxymethyl) acrylate, and methyl 2-(phenoxymethyl)-acrylate had extrapolated [M]_{eq} = 0.6-0.7 M, and 0.19 M, respectively, at a temperature of 60°C which is significantly higher than the [M]_{eq} of most methacrylates at the same temperature (ca. 0.01 M). 86,87 Radical polymerizations of 20EOAM monomers with shorter ethylene oxide repeat units (n = 1, 2, and 3) in the α -position were also faster than RP of

^bBased upon conversion (p) by ¹HNMR.

^cTaken as the slope of the first order kinetic plot in Figure 7C in the first 24 h of the reaction.

^dRelative to linear PMMA standards using GPC with DMF eluent.

eWeight fraction of polymeric fraction determined by peak fitting of GPC traces using Origin software. Peak fits are provided in the Supplementary Information (Figure S26).

f[M]/[TTC] = 22/1.

^gThe $k_{p,app}$ is taken as the slope of the first order kinetic plot up to 4 h.

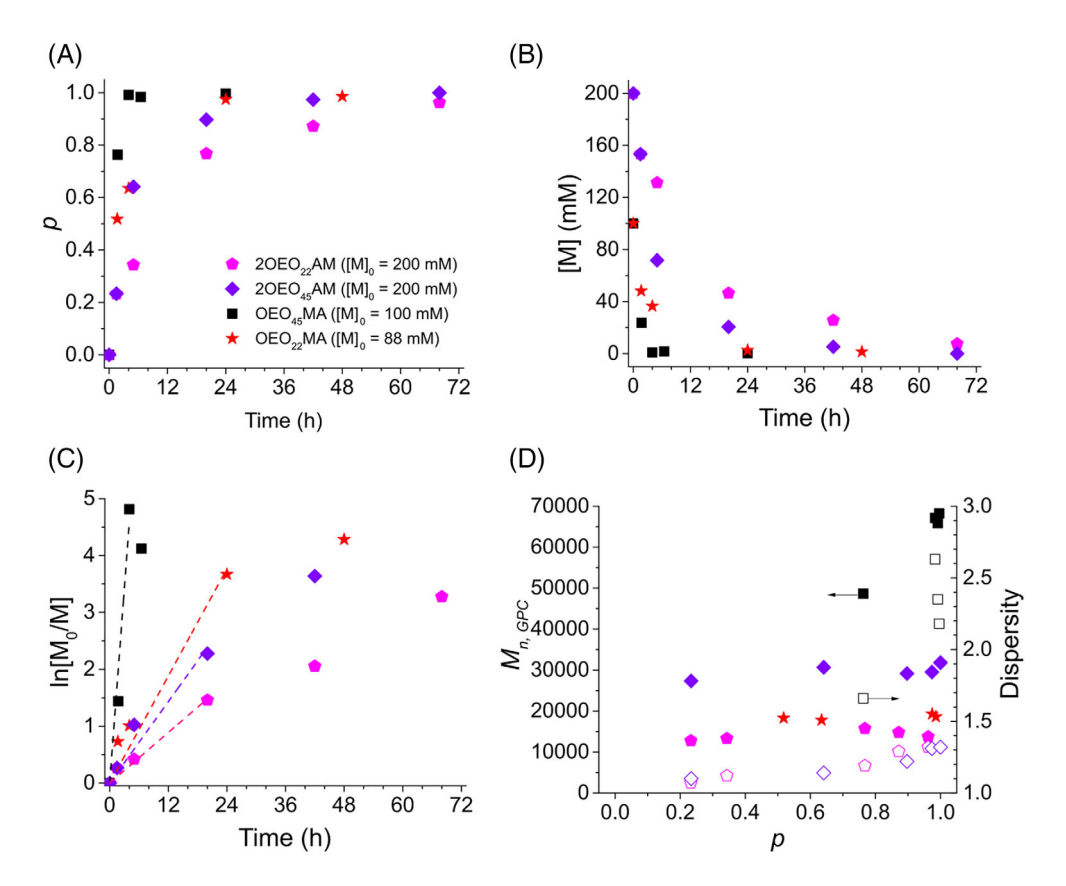


FIGURE 7 Grafting-through polymerization of $OEO_{22}MA$, $OEO_{45}MA$, $2OEO_{22}AM$, and $2OEO_{45}AM$ by photoinduced energy/electron transfer-reversible addition-fragmentation chain transfer. (A) Kinetic plot of conversion versus reaction time. (B) Kinetic plot of monomer concentration versus time. (C) First order kinetic plot. The dotted lines are linear fits of the datapoints before 24 h, with a set y-intercept = 0. The slope of the line is given as the $k_{p,app}$ in Table 2. (D) Molecular weight and dispersity versus conversion plot. The molecular weight of all samples are given relative to linear PMMA standards in DMF. Conditions: $OEO_{22}MA$ was polymerized at $[M]_0 = 88$ mM with 107 ppm of Ru catalyst and a TTC CTA; $OEO_{45}MA$ was polymerized at $[M]_0 = 100$ mM with 94 ppm of Ru catalyst and a TTC CTA; $2OEO_{22}AM$ was polymerized at $[M]_0 = 200$ mM with 94 ppm of Ru catalyst and a TTC CTA. All reactions were conducted in 20 vol% DMF, with the remaining volume occupied by monomer and D_2O . Reactions were started upon exposure to blue light without prior degassing, at a temperature of 35°C

MMA, but had no observable equilibrium monomer concentrations under similar conditions. ⁸⁸ Indeed, degassed photoiniferter RAFT polymerizations of $OEO_{22}MA$ and $OEO_{45}MA$ at $85^{\circ}C$ polymerized to final [M] ~ 10 –20 mM, but the inverted $2OEO_{45}AM$ plateaued at a [M] = 170 mM, indicating there are noticeable thermodynamic differences between the isomeric OEO macromonomers at elevated temperature (Figure S17).

The kinetics of grafting-through PET-RAFT polymerization of OEO₄₅MA, 2OEO₂₂AM and 2OEO₄₅AM were compared using a recipe of $[M]_0/[TTC]_0 = 25/1$ with 94 ppm of catalyst at an identical initial monomer concentration of 100 mM. The steady-state rate of PET-RAFT is a product of [M], the rate constant of propagation, k_p , and the steady state radical concentration (Equation 3). The steady state radical concentration in a PET-RAFT is the square root ratio of the rate of radical generation by the photocatalyst (R_i) to the rate constant of termination,

 $k_{\rm t}$, plus the term $k_{\rm t,cross}K_{\rm RAFT}[{\rm CTA}]$ to account for retardation caused by cross-termination with the RAFT intermediate radical. ^{89,90} The rate constant, $k_{\rm t,cross}$, is the cross-termination rate constant, $K_{\rm RAFT}$ is the RAFT equilibrium constant, and [CTA] is the CTA concentration.

$$R_{\rm p} = k_{\rm p}[M][P] = k_{\rm p}[M] \sqrt{\frac{R_{\rm i}}{k_{\rm t} + k_{\rm t,cross} K_{\rm RAFT}[{\rm CTA}]}}$$
 (3)

$$ln \frac{[M]_0}{[M]} = k_p[P]t = k_{p,app}t$$
(4)

We compare the polymerizations of these monomers wholistically using an observed apparent rate of propagation, $k_{\rm p,app}$, extrapolated as the slope of the first order kinetic plots in Figure 7 which encompasses differences in $k_{\rm p}/k_{\rm t}^{0.5}$ and RAFT retardation. (Equation 4).

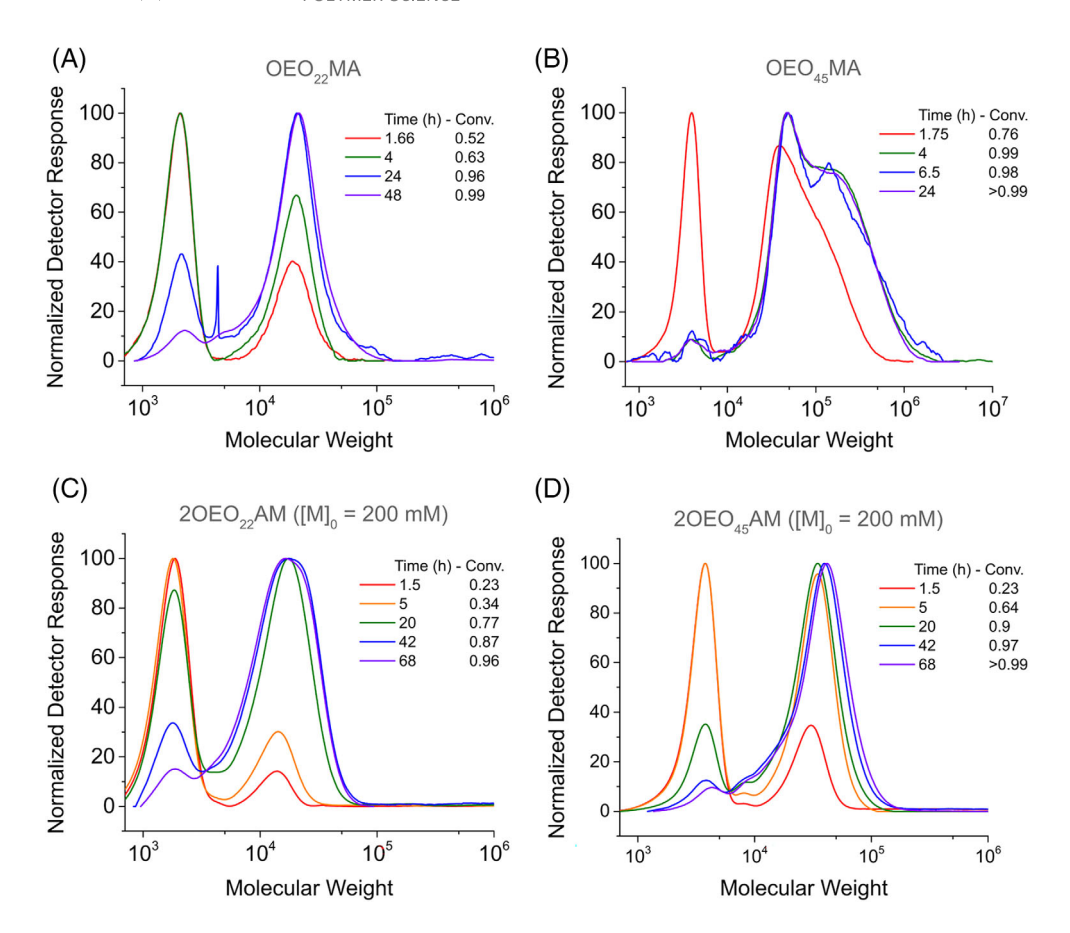


FIGURE 8 Gel permeation chromatography (GPC) traces of the grafting-through polymerization of (A) OEO₂₂AM at $[M]_0 = 88 \text{ mM}$ with 107 ppm of Ru catalyst and a trithiocarbonate 4-((([2-carboxyethyl]thio) carbonothioyl)thio)-4-cyanopentanoic acid (TTC) CTA. Target DP = 22; (B) OEO₄₅MA at $[M]_0 = 100 \text{ mM}$ with 94 ppm of Ru catalyst and a TTC CTA. Target DP = 25; (C) $2OEO_{22}AM$ at $[M]_0 = 200 \text{ mM}$ with 94 ppm of Ru catalyst and a TTC CTA. Target DP = 25; (D) $2OEO_{45}AM$ at $[M]_0 = 200 \text{ mM}$ with 94 ppm of Ru catalyst and a TTC CTA. Target DP = 25. The reactions were conducted under blue light irradiation ($\lambda = 465$ nm, 6.5 mW/cm²) at a temperature of 35°C. the conditions are given in Table 2

The PET-RAFT of the longer OEO₄₅MA macromonomer proceeded with linear first order kinetics to quantitative conversion in under 24 h with poor control (2KMA-94, Figure 7). The $k_{p,app}$ of the polymerization was more than seven times higher than the polymerization of the shorter OEO₂₂MA macromonomer under comparable conditions. The faster polymerization of bulkier OEO monomers within the same monomer class agrees with the observed increase in $k_p/k_t^{0.5}$ for *n*-alkyl methacrylates with longer sidechains. 91 The GPC traces of P(OEO₄₅MA) were ill-defined, with bimodal molecular weight distribution and high molecular weight shoulder, suggesting inefficient exchange of the TTC (i.e. lower K_{RAFT} and plausibly $k_{t,cross}$) also contributed to the faster rate of polymerization (Figure 8). The normal ATRP of OEO₄₅MA at various temperatures and $[M]_0$ in anisole was also poorly controlled, which confirms the longer side-chain OEO₄₅MA is still difficult to polymerize with sufficient control via RDRP. 43

The polymerization of $20EO_{22}AM$ at $[M]_0 = 100$ mM was significantly slower than the standard OEOMA monomers, with a $k_{\rm p,app}$ five times lower than the polymerization of $0EO_{22}MA$. The longer $20EO_{45}AM$ macromonomer was slightly faster. The $k_{\rm p,app}$ of $20EO_{45}AM$ polymerization by PET-RAFT was four times lower than that of $0EO_{22}MA$, and 29 times lower than

OEO $_{45}$ MA (Figure S24). Both polymerizations reached 46% and 52% conversion, respectively, in 24 h and had negligible polymerization over the next 48 h (Table 2, Figure S24). The products had relatively low dispersity <1.2, with low molecular weight tailing appearing in the GPC traces between the 24 and 72 h timepoints (Figure S25).

The improved control over RAFT polymerization suggests the exchange of RAFT agent was efficient for the 20EOAM macromonomers, including the longer 20EO₄₅AM, which might have slowed the overall rate of polymerization. The dispersity 20EO₂₂AM polymerizations at comparable conversion were lower than those of 0EO₂₂MA, suggesting more efficient exchange of the CTA with the inverted macromonomers. The difference in polymerization control is more obvious between the longer 20EO₄₅AM and 0EO₄₅MA, where the former maintained a low $\mathcal{D} < 1.2$ until the reaction plateaued at 60% conversion and the latter rapidly polymerized to high $\mathcal{D} = 2.18$ with bimodal molecular weight distribution.

The faster rate of polymerization of 2OEO₄₅AM relative to 2OEO₂₂AM agrees with the increase in rate of polymerization for OEO₄₅MA relative to OEO₂₂MA, however control was maintained for the inverted macromonomers. This confirms an increase in rate of RAFT

polymerization with sidechain length for monomers with the same substituents around the olefin, which may include contributions from a higher $k_p/k_t^{0.5}$ for the bulkier macromonomers and a less efficient RAFT exchange.

The molar concentration of all reagents was doubled for 2OEO₂₂AM and 2OEO₄₅AM polymerizations, scaled to $[M]_0 = 200$ mM, by reducing the volume fraction of water. This effectively doubled the molar concentration of catalyst and chain transfer agent, while the solid loading of 2OEO₂₂AM macromonomer increased from 10 vol% at $[M]_0 = 100 \text{ mM}-20 \text{ vol}\%$ at $[M]_0 = 200 \text{ mM}$, and the volume fraction of 2OEO₄₅AM increased from 20 to 40 v/v% for the same respective concentrations. The volume fraction of DMF was maintained at 20 vol%. It should be noted that the rate constant of propagation (k_p) in a dilute (5 wt%) aqueous polymerization of OEO₇₋₈MA was a factor of \sim 7 times higher relative to a polymerization in bulk.⁹² Doubling the concentration of all reagents increased the concentration of propagating centers and increased the $k_{p,app}$ of $20EO_{22}AM$ and $20EO_{45}AM$ polymerizations by a factor 2.3 and 3, respectively, relative to the polymerizations at half the concentration. The overall effect of increasing the concentration of inverted macromonomer, catalyst, and TTC outweighed the kinetic penalties of the less polar reaction medium under the tested conditions (Figure 7).

 $2 \text{OEO}_{22} \text{AM}$ polymerization reached 87% conversion after 42 h, while polymerization of $2 \text{OEO}_{45} \text{AM}$ with the longer OEO chain was faster and reached 97% conversion in the same amount of time. Indeed, the $k_{\text{p,app}}$ of the $2 \text{OEO}_{45} \text{AM}$ polymerization at $[\text{M}]_0 = 200 \text{ mM}$ was ~ 2 times larger than the $k_{\text{p,app}}$ of the $2 \text{OEO}_{22} \text{AM}$ polymerization under otherwise comparable conditions. This agrees with the faster rate of polymerization for PET-RAFT of the longer $0 \text{EO}_{45} \text{MA}$ macromonomer relative to the $0 \text{EO}_{22} \text{MA}$ macromonomer with shorter sidechain, however to a smaller extent. Polymerizations of both monomers eventually reached > 95% conversion after 68 h of blue light irradiation.

The molecular weight versus conversion plot showed a decrease in bottlebrush molecular weight and increase in dispersity in the polymerization of $2\text{OEO}_{22}\text{AM}$ (Figure 7D). The molecular weight of the bottlebrush peaked at a $M_{\text{n,GPC}}=15,750$ at 77% conversion after 20 h of irradiation. The molecular weight dropped to a final $M_{\text{n,GPC}}=13,750$, and dispersity increased from 1.19 to 1.32, as the polymerization continued to 96% conversion after a total of 68 h. The molecular weight of P ($20\text{EO}_{45}\text{AM}$) plateaued near a $M_{\text{n,GPC}}\sim30,000$ after the reaction reached 64% conversion. The dispersity of the bottlebrush increased with conversion from 1.14 to 1.32 once the reaction reached quantitative conversion by ^1H NMR. The decrease in molecular weight in both

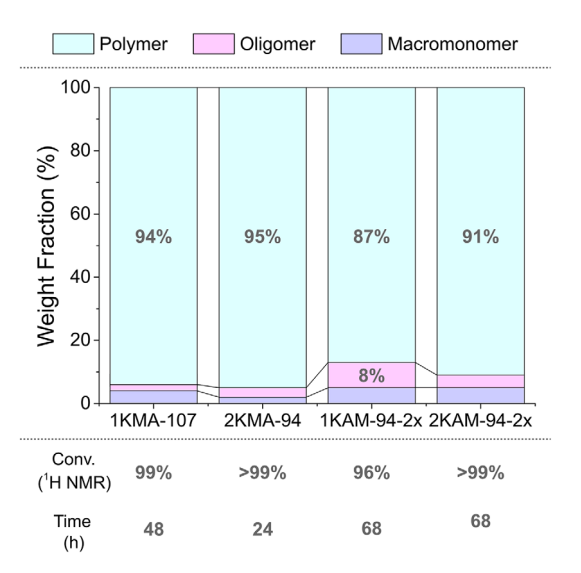


FIGURE 9 Bar graph of polymer weight fractions in the final GPC trace of experiments 1KMA-107, 2KMA-94, 1KAM-94-2X, and 2KAM-94-2X. The weight fractions were found by multiple peak fitting to the bottlebrush (BB), oligomer (Olig), and macromonomer (MM) peaks in units of elution volume versus normalized refractive index detector response. The peak areas of the bottlebrush (A_{BB}) , oligomers (A_{Olig}), macromonomer (A_{MM}), and solvent (A_{solv}) were obtained by multiple peak fitting to the respective peaks in the crude GPC trace. The weight fractions of the bottlebrush (φ_{BB}), oligomers (ϕ_{Olig}), and macromonomer (ϕ_{MM}) are given by the ratio of the peak area to the sum of all polymeric peak areas times 100. The experimental conditions used in the experiments are given in Table 2. The peak fits and area of each peak are provided in the Supplementary Information. The conversion data from ¹H NMR and time points are given under the bar graph

experiments may be attributed to degradation of the CTA leading to high molecular weight chains lacking CEF and impurities which can initiate formation of new oligomers.

Multiple peak fitting of the GPC traces provided insight into the discrepancies between the molecular weight distributions and conversion by ¹H NMR. The weight fraction of monomer, oligomers, and bottlebrushes were determined by multiple peak fitting of the GPC traces using the refractive index versus elution volume plot (Figure S26). The weight fraction of each peak is reported as the ratio of polymer peak area divided by the total peak area of all species. The peak fitting shows conversion by GPC underestimated macromonomer conversion relative to the conversion reported by ¹H NMR, with the conversion by ¹H NMR consistently >2% higher than the conversion by GPC (Table 2). Indeed, the polymerization 2KAM-94-2x reached quantitative conversion by ¹H NMR but contained 5 wt% of residual "macromonomer" in the final crude GPC trace. This can be explained by incomplete

functionalization of the OEO macromonomers, or by loss of functionality via a slow chain breaking reaction (transfer/termination) in a fraction of macromonomers.

The macromonomers with a faster rate of polymerization generally contained a lower weight fraction of oligomers than the slower polymerizing macromonomers (Figure 6). The 2KMA-94 polymerization was the fastest, reaching 99% conversion in 4 h, and only contained 3 wt% oligomers in the peak fitting. This was comparable to the 2 wt% weight fraction of oligomers obtained in the polymerization of OEO₂₂MA in experiment 1KMA-107. The weight fraction of oligomers obtained in the polymerization of the long "inverted" 2OEO₄₅AM macromonomer was 4%. The polymerization of 2OEO₂₂AM was the slowest and had a high 10 wt% fraction of oligomer impurities (Figure 9).

3 | CONCLUSIONS

controlled radical polymerizations of Aqueous oligo(ethylene oxide) monomethyl ether methacrylate (OEOMA) and "inverted" methyl 2-(oligo(ethylene oxide) monomethyl ether)acrylate (20EOAM) macromonomers were conducted without prior degassing using PET RAFT. The inverted 20EOAM macromonomers had the OEO sidechain installed in the alpha-position to better understand the effects of monomer sterics of graftingthrough radical polymerizations of 1,1-disubstituted acrylic macromonomers. The PET-RAFT of the macromonomers was conducted at low [M]₀/[CTA]₀ molar ratio with deoxygenation using a Ru catalyst to maintain polymerization. Polymerizations of all macromonomers reached near quantitative monomer conversion.

The macromonomers with longer sidechains polymerized faster than those with shorter sidechains within the same monomer class. The longer OEO₄₅MA macromonomer had an apparent rate constant of polymerization seven times larger than the OEO₂₂MA macromonomer with a shorter sidechain. The rates of polymerization were significantly slower for the inverted macromonomers, however the same trend was observed. The inverted macromonomers polymerized 4-5 times slower than $OEO_{22}MA$ at a $[M]_0 = 100$ mM. The polymerization of longer 2OEO₄₅AM was a factor of three times faster than 2OEO22AM when the initial monomer concentration was increased to $[M]_0 = 200$ mM. This suggests the addition of the alpha substituent significantly slows the polymerization of OEO macromonomers, and longer sidechains with similar sterics around the olefin can led to an overall faster polymerization at the same molar concentration. The observed faster polymerization

of bulkier OEO monomers within the same monomer class agrees with the reported increase in $k_{\rm p}/k_{\rm t}^{0.5}$ for n-alkyl methacrylates with longer sidechains, 91 however differences in RAFT exchange may also contribute to the overall differences in polymerization rate as evidenced by poor control observed in the polymerization of OEO₄₅MA.

The slower rate of polymerization led to tailing during the grafting-through polymerizations. The tailing may be attributed to degradation of the trithiocarbonate end-groups after prolonged exposure to blue light irradiation in water. The degree of tailing and oligomerization observed in the GPC traces may be avoided by increasing the rate of polymerization, similar to the strategy used to polymerize acrylamides by an aqueous RAFT process. 93,94

ACKNOWLEDGMENTS

This manuscript is dedicated to Professor Klaus Muellen on the occasion of his 75th birthday.

Financial support from the National Science Foundation through NSF DMR 1921858 and NSF DMR 2202747 is acknowledged. MM acknowledges support from the Harrison Fellowship (CMU Department of Chemistry). The NMR Facility at Carnegie Mellon University was partially supported by the NSF (CHE-0130903, CHE-1039870, and CHE-1726525).

CONFLICT OF INTEREST

The authors declare no conflict of interest.

ORCID

Krzysztof Matyjaszewski https://orcid.org/0000-0003-1960-3402

REFERENCES

- [1] M. Abbasi, L. Faust, M. Wilhelm, Adv. Mater. 2019, 31, 1806484
- [2] Z. Li, M. Tang, S. Liang, M. Zhang, G. V. Biesold, Y. He, S. Hao, W. Choi, Y. Liu, J. Peng, Prog. Polym. Sci. 2021, 116, 101387.
- [3] G. Xie, M. R. Martinez, M. Olszewski, S. S. Sheiko, K. Matyjaszewski, Biomacromolecules 2018, 20, 27.
- [4] R. Verduzco, X. Li, S. L. Pesek, G. E. Stein, Chem. Soc. Rev. 2015, 44, 2405.
- [5] J. Rzayev, ACS Macro Lett, 2012, 1, 1149.
- [6] S. S. Sheiko, B. S. Sumerlin, K. Matyjaszewski, *Prog. Polym. Sci.* 2008, 33, 759.
- [7] H.-I. Lee, J. Pietrasik, S. S. Sheiko, K. Matyjaszewski, Prog. Polym. Sci. 2010, 35, 24.
- [8] J. M. Chan, A. C. Kordon, R. Zhang, M. Wang, Proc. Natl. Acad. Sci. 2021, 118, e2109534118.
- [9] S. Rathgeber, T. Pakula, A. Wilk, K. Matyjaszewski, K. L. Beers, J. Chem. Phys. 2005, 122, 124904.

- [10] I. N. Haugan, M. J. Maher, A. B. Chang, T.-P. Lin, R. H. Grubbs, M. A. Hillmyer, F. S. Bates, ACS Macro Lett. 2018, 7 525
- [11] H. Liang, Z. Wang, S. S. Sheiko, A. V. Dobrynin, *Macromole-cules* 2019, 52, 3942.
- [12] H. Liang, B. J. Morgan, G. Xie, M. R. Martinez, E. B. Zhulina, K. Matyjaszewski, S. S. Sheiko, A. V. Dobrynin, *Macromole-cules* 2018, 51, 10028.
- [13] Y. Xia, V. Adibnia, C. Shan, R. Huang, W. Qi, Z. He, G. Xie, M. Olszewski, G. De Crescenzo, K. Matyjaszewski, *Langmuir* 2019, 35, 15535.
- [14] Y. Xia, V. Adibnia, R. Huang, F. Murschel, J. Faivre, G. Xie, M. Olszewski, G. De Crescenzo, W. Qi, Z. He, Am. Ethnol. 2019, 131, 1322.
- [15] X. Banquy, J. Burdyńska, D. W. Lee, K. Matyjaszewski, J. Israelachvili, J. Am. Chem. Soc. 2014, 136, 6199.
- [16] R. Yuan, M. Kopeć, G. Xie, E. Gottlieb, J. W. Mohin, Z. Wang, M. Lamson, T. Kowalewski, K. Matyjaszewski, *Polymer* 2017, 126, 352.
- [17] G. Xie, X. Lin, M. R. Martinez, Z. Wang, H. Lou, R. Fu, D. Wu, K. Matyjaszewski, *Chem. Mater.* 2018, 30, 8624.
- [18] X. Lin, G. Xie, S. Liu, M. R. Martinez, Z. Wang, H. Lou, R. Fu, D. Wu, K. Matyjaszewski, ACS Appl. Mater. Interfaces 2019, 11, 18763.
- [19] G. Xie, P. Krys, R. D. Tilton, K. Matyjaszewski, *Macromole-cules* 2017, 50, 2942.
- [20] T.-L. Hsieh, M. R. Martinez, S. Garoff, K. Matyjaszewski, R. D. Tilton, J. Colloid Interface Sci. 2021, 581, 135.
- [21] B. Wang, T. Liu, H. Chen, B. Yin, Z. Zhang, T. P. Russell, S. Shi, Am. Ethnol. 2021, 133, 19778.
- [22] M. Müllner, Macromol. Chem. Phys. 2016, 217, 2209.
- [23] W. Raj, K. Jerczynski, M. Rahimi, A. Przekora, K. Matyjaszewski, J. Pietrasik, Mater. Sci. Eng. C 2021, 130, 112439.
- [24] M. Rahimi, G. Charmi, K. Matyjaszewski, X. Banquy, J. Pietrasik, Acta Biomater. 2021, 123, 31.
- [25] W. F. Daniel, J. Burdyńska, M. Vatankhah-Varnoosfaderani, K. Matyjaszewski, J. Paturej, M. Rubinstein, A. V. Dobrynin, S. S. Sheiko, *Nat. Mater.* 2016, 15, 183.
- [26] V. G. Reynolds, S. Mukherjee, R. Xie, A. E. Levi, A. Atassi, T. Uchiyama, H. Wang, M. L. Chabinyc, C. M. Bates, *Mater. Horiz.* 2020, 7, 181.
- [27] J. L. Self, C. S. Sample, A. E. Levi, K. Li, R. Xie, J. R. de Alaniz, C. M. Bates, J. Am. Chem. Soc. 2020, 142, 7567.
- [28] M. Vatankhah-Varnosfaderani, W. F. Daniel, M. H. Everhart, A. A. Pandya, H. Liang, K. Matyjaszewski, A. V. Dobrynin, S. S. Sheiko, *Nature* 2017, 549, 497.
- [29] F. Vashahi, M. R. Martinez, E. Dashtimoghadam, F. Fahimipour, A. N. Keith, E. A. Bersenev, D. A. Ivanov, E. B. Zhulina, P. Popryadukhin, K. Matyjaszewski, Sci. Adv. 2022, 8, eabm2469.
- [30] Y. Cong, M. Vatankhah-Varnosfaderani, V. Karimkhani, A. N. Keith, F. A. Leibfarth, M. R. Martinez, K. Matyjaszewski, S. S. Sheiko, *Macromolecules* 2020, 53, 8324.
- [31] K. L. Beers, S. G. Gaynor, K. Matyjaszewski, S. S. Sheiko, M. Möller, *Macromolecules* 1998, 31, 9413.
- [32] W. Hou, Z. Li, L. Xu, Y. Li, Y. Shi, Y. Chen, ACS Macro Lett. 2021, 10, 1260.
- [33] G. Xie, M. R. Martinez, W. F. M. Daniel, A. N. Keith, T. G. Ribelli, M. Fantin, S. S. Sheiko, K. Matyjaszewski, *Macromole-cules* 2018, 51, 6218.

- [34] M. R. Martinez, J. Sobieski, F. Lorandi, M. Fantin, S. Dadashi-Silab, G. Xie, M. Olszewski, X. Pan, T. G. Ribelli, K. Matyjaszewski, *Macromolecules* 2020, 53, 59.
- [35] J. Tanaka, S. Häkkinen, P. T. Boeck, Y. Cong, S. Perrier, S. S. Sheiko, W. You, Am. Ethnol. 2020, 132, 7270.
- [36] H. Gao, K. Matyjaszewski, J. Am. Chem. Soc. 2007, 129, 6633.
- [37] L. A. Navarro, T. P. Shah, S. Zauscher, Langmuir 2020, 36, 4745.
- [38] K. Kawamoto, M. Zhong, K. R. Gadelrab, L.-C. Cheng, C. A. Ross, A. Alexander-Katz, J. A. Johnson, J. Am. Chem. Soc. 2016, 138, 11501.
- [39] W. J. Neary, T. A. Isais, J. G. Kennemur, J. Am. Chem. Soc. 2019, 141, 14220.
- [40] M. R. Martinez, Y. Cong, S. S. Sheiko, K. Matyjaszewski, ACS Macro Lett. 2020, 9, 1303.
- [41] L. Fournier, D. M. Rivera Mirabal, M. A. Hillmyer, Macromolecules 2022, 55, 1003.
- [42] A. E. Levi, J. Lequieu, J. D. Horne, M. W. Bates, J. M. Ren, K. T. Delaney, G. H. Fredrickson, C. M. Bates, *Macromolecules* 2019, 52, 1794.
- [43] H. Y. Cho, P. Krys, K. Szcześniak, H. Schroeder, S. Park, S. Jurga, M. Buback, K. Matyjaszewski, *Macromolecules* 2015, 48, 6385.
- [44] T. G. Floyd, S. Häkkinen, M. Hartlieb, A. Kerr, S. Perrier, RAFT Polymerization: Methods, Synthesis and Applications, 2021, 2, 933.
- [45] V. Raus, E. Čadová, L. Starovoytova, M. Janata, Macromolecules 2014, 47, 7311.
- [46] M. J. Flanders, W. M. Gramlich, Polym. Chem. 2018, 9, 2328.
- [47] M. R. Martinez, P. Krys, S. S. Sheiko, K. Matyjaszewski, ACS Macro Lett. 2020, 9, 674.
- [48] A. Zhang, K. Jung, A. Li, J. Liu, C. Boyer, Prog. Polym. Sci. 2019, 99, 101164.
- [49] C. Weber, R. Hoogenboom, U. S. Schubert, Prog. Polym. Sci. 2012, 37, 686.
- [50] B. Peng, N. Grishkewich, Z. Yao, X. Han, H. Liu, K. C. Tam, ACS Macro Lett. 2012, 1, 632.
- [51] V. Klimkevicius, T. Graule, R. Makuska, *Langmuir* 2015, 31, 2074.
- [52] S.-I. Yamamoto, J. Pietrasik, K. Matyjaszewski, Macromolecules 2008, 41, 7013.
- [53] S.-I. Yamamoto, J. Pietrasik, K. Matyjaszewski, J. Polym. Sci., Part A: Polym. Chem. 2008, 46, 194.
- [54] S.-I. Yamamoto, J. Pietrasik, K. Matyjaszewski, Macromolecules 2007, 40, 9348.
- [55] Y. Zhuang, Y. Su, Y. Peng, D. Wang, H. Deng, X. Xi, X. Zhu, Y. Lu, Biomacromolecules 2014, 15, 1408.
- [56] V. Klimkevicius, R. Makuska, Eur. Polym. J. 2017, 86, 94.
- [57] Z. Cheng, X. Zhu, E. Kang, K. Neoh, Langmuir 2005, 21, 7180
- [58] T. Krivorotova, A. Vareikis, D. Gromadzki, M. Netopilík, R. Makuška, Eur. Polym. J. 2010, 46, 546.
- [59] J. K. Oh, K. Min, K. Matyjaszewski, Macromolecules 2006, 39, 3161.
- [60] H. S. Wang, N. P. Truong, Z. Pei, M. L. Coote, A. Anastasaki, J. Am. Chem. Soc. 2022, 144, 4678.
- [61] F. García-Martín, M. Quintanar-Audelo, Y. García-Ramos, L. J. Cruz, C. Gravel, R. Furic, S. Côté, J. Tulla-Puche, F. Albericio, J. Comb. Chem. 2006, 8, 213.

- [62] Y. García-Ramos, M. Paradís-Bas, J. Tulla-Puche, F. Albericio, J. Pept. Sci. 2010, 16, 675.
- [63] J. Xu, K. Jung, C. Boyer, Macromolecules 2014, 47, 4217.
- [64] J. Xu, K. Jung, N. A. Corrigan, C. Boyer, Chem. Sci. 2014, 5, 3568.
- [65] J. Niu, Z. A. Page, N. D. Dolinski, A. Anastasaki, A. T. Hsueh, H. T. Soh, C. J. Hawker, ACS Macro Lett. 2017, 6, 1109.
- [66] D. J. Walsh, M. A. Wade, S. A. Rogers, D. Guironnet, *Macro-molecules* 2020, 53, 8610.
- [67] Q. Fu, K. Xie, T. McKenzie, G. Qiao, Polym. Chem. 2017, 8, 1519.
- [68] J. R. Lamb, K. P. Qin, J. A. Johnson, Polym. Chem. 2019, 10, 1585.
- [69] J. Yeow, R. Chapman, A. J. Gormley, C. Boyer, Chem. Soc. Rev. 2018, 47, 4357.
- [70] J. Christmann, A. Ibrahim, V. Charlot, C. Croutxé-Barghorn, C. Ley, X. Allonas, *ChemPhysChem* 2016, 17, 2309.
- [71] N. Corrigan, J. Xu, C. Boyer, X. Allonas, *ChemPhotoChem* 2019, 3, 1193.
- [72] C. K. Prier, D. A. Rankic, D. W. C. MacMillan, Chem. Rev. 2013, 113, 5322.
- [73] Y. Cheng, J. Yang, Y. Qu, P. Li, Org. Lett. 2012, 14, 98.
- [74] Y. Q. Zou, J. R. Chen, X. P. Liu, L. Q. Lu, R. L. Davis, K. A. Jørgensen, W. J. Xiao, Am. Ethnol. 2012, 124, 808.
- [75] B. H. Bielski, D. E. Cabelli, R. L. Arudi, A. B. Ross, J. Phys. Chem. Ref. Data 1985, 14, 1041.
- [76] Y. Che, M. Tsushima, F. Matsumoto, T. Okajima, K. Tokuda, T. Ohsaka, J. Phys. Chem. 1996, 100, 20134.
- [77] R. Cox, J. Burrows, J. Phys. Chem. 1979, 83, 2560.
- [78] Y. Lv, Z. Liu, A. Zhu, Z. An, J. Polym. Sci., Part A: Polym. Chem. 2017, 55, 164.
- [79] A. Reyhani, M. D. Nothling, H. Ranji-Burachaloo, T. G. McKenzie, Q. Fu, S. Tan, G. Bryant, G. G. Qiao, Angew. Chem. Int. Ed. 2018, 57, 10288.
- [80] T. McKenzie, L. D. M. Costa, Q. Fu, D. Dunstan, G. Qiao, Polym. Chem. 2016, 7, 4246.
- [81] J. F. Quinn, L. Barner, C. Barner-Kowollik, E. Rizzardo, T. P. Davis, Macromolecules 2002, 35, 7620.

- [82] A. V. Fuchs, K. J. Thurecht, ACS Macro Lett. 2017, 6, 287.
- [83] J. Rzayev, J. Penelle, J. Polym. Sci., Part A: Polym. Chem. 2002, 40, 836
- [84] B. Yamada, S. Kobatake, Prog. Polym. Sci. 1994, 19, 1089.
- [85] S. Kobatake, B. Yamada, Polym. J. 1996, 28, 535.
- [86] B. Yamada, M. Satake, T. Otsu, Macromol. Chem. Phys. 1991, 192, 2713.
- [87] B. Yamada, M. Satake, T. Otsu, Polym. J. 1992, 24, 563.
- [88] B. Yamada, S. Kobatake, S. Aoki, J. Polym. Sci., Part A: Polym. Chem. 1993, 31, 3433.
- [89] K. G. E. Bradford, L. M. Petit, R. Whitfield, A. Anastasaki, C. Barner-Kowollik, D. Konkolewicz, J. Am. Chem. Soc. 2021, 143, 17769.
- [90] P. N. Kurek, A. J. Kloster, K. A. Weaver, R. Manahan, M. L. Allegrezza, N. De Alwis Watuthanthrige, C. Boyer, J. A. Reeves, D. Konkolewicz, *Ind. Eng. Chem. Res.* 2018, 57, 4203.
- [91] S. Beuermann, M. Buback, Prog. Polym. Sci. 2002, 27, 191.
- [92] S. Smolne, S. Weber, M. Buback, Macromol. Chem. Phys. 2016, 217, 2391.
- [93] C. L. McCormick, A. B. Lowe, Acc. Chem. Res. 2004, 37, 312.
- [94] A. W. Fortenberry, C. L. McCormick, A. E. Smith, RAFT Polymerization: Methods, Synthesis and Applications 2, 2021, 2, 679.

SUPPORTING INFORMATION

Additional supporting information may be found in the online version of the article at the publisher's website.

How to cite this article: M. R. Martinez, S. Dworakowska, A. Gorczyński, G. Szczepaniak, F. D. L. Bossa, K. Matyjaszewski, *J. Polym. Sci.* **2022**, *60*(12), 1887. https://doi.org/10.1002/pol.20220086